ELSEVIER

Nuclear Instruments and Methods in Physics Research B 157 (1999) 291–296

NIM B
Beam Interactions with Materials & Atoms

www.elsevier.nl/locate/nimb

Submonolayer homoepitaxy on Fe(1 0 0) studied by grazing ion–surface scattering: experiments and computer simulations

R. Pfandzelter *

Humboldt-Universität zu Berlin, Institut für Physik, Invalidenstrasse 110, 10115 Berlin, Germany

Abstract

Grazing ion-surface scattering is used to study in real space and real time epitaxial growth processes. By example of 25 keV He^+-ions scattered during submonolayer homoepitaxy on Fe(1 0 0), we show that an interpretation of experiments is straightforward by means of classical mechanics computer simulations. A fit of intensity and angular profile of the specular beam allow one to deduce basic quantities like the island density. © 1999 Elsevier Science B.V. All rights reserved.

PACS: 79.20.Rf; 79.20.Ap; 68.55.-a
Keywords: Medium energy ion scattering; Low index single crystal surfaces; Iron; Computer simulations; Single crystal epitaxy; Surface structure, morphology, roughness, and topography; Ion–solid interactions

1. Introduction

Diffraction techniques like reflection high energy electron diffraction (RHEED), low energy electron diffraction (LEED) or atom beam diffraction have become powerful tools to monitor and control epitaxial growth with submonolayer precision. In general information is deduced from intensity and angular profile of the specular-beam. The measurements can often be performed in situ and in real time, thus avoiding possible distortions due to sample transfers, temperature quenching, or replica techniques [1] and stand out for their superior statistics compared with imaging techniques such as scanning tunneling microscopy (STM) [2].

LEED [2–6] and atom beam diffraction [1,7,8] have been profitably exploited to deduce growth related morphological quantities like island size and separation, which are linked by atomistic nucleation theory [9] and Monte Carlo simulations to basic quantities such as activation energies and critical island size. For coverages from about 0.2–0.6 monolayers (ML) diffraction patterns show characteristic side bands. Their position reflects a length L, which is attributed to the island separation and related to the island density N via $L \approx 1/\sqrt{N}$. The island density has been found to be almost constant, as it is expected for this coverage range, where adatoms deposited attach to existing islands and no additional islands nucleate

* Tel.: +49-30-2093-7693; fax: +49-30-2093-7899; e-mail: pfandz@physik.hu-berlin.de

0168-583X/99/$ – see front matter © 1999 Elsevier Science B.V. All rights reserved.
PII: S 0 1 6 8 - 5 8 3 X (9 9) 0 0 4 4 6 - 2

(aggregation regime) [10]. Moreover, using two-level models for the covered surface, the distribution of island size and separation could be inferred from fits of calculated to measured angular profiles [4].

As an alternative to diffraction techniques working in reciprocal-space, grazing scattering of fast ions has been introduced as a real-space technique [11–13]. For scattering from a flat surface the trajectories of ions are governed by correlated series of small angle collisions with surface-layer atoms, which leads to specular reflection. During epitaxial growth the ions will hit steps forming the boundaries of islands. This perturbs the scattering process resulting in a loss of specular-beam intensity. Treatment of the scattering process by classical mechanics facilitates interpretation of measurements by means of computer simulations emulating ion trajectories [14].

In the present work we address the question how information on morphological quantities can be obtained from measurements on grazing ion scattering during epitaxial growth. A comparison between experiments and computer simulations will reveal benefits and limitations of the technique. We study the scattering of 25 keV He^+-ions during submonolayer homoepitaxial growth of Fe on Fe(1 0 0). This system is considered as a model system, since it avoids complications like reconstruction, alloying, or strain. It has been studied both experimentally by STM [15,16] and theoretically [17,18].

2. Experiment

The experimental setup is described in Refs. [19,20]. In brief, a well collimated beam of 25 keV He^+-ions is directed upon a (1 0 0) surface of an Fe single crystal disk at a polar angle $\Phi_{in} = 1.5°–2°$ to the surface plane and an azimuthal angle Θ_{in} of a few degrees to the [0 0 1] surface lattice direction. Projectiles scattered in the forward direction within the plane spanned by the ion beam and the surface normal are detected by a channeltron detector. The detector can be moved in the scattering plane to measure the one-dimensional (1D) angular profile of the specular beam.

In situ preparation of the target surface is performed by grazing Ar^+-sputtering and subsequent annealing. The residual surface step density can be chosen, within certain limits, by the annealing temperature. A flat surface (average separation of steps >2000 Å) is obtained at 920 K, whereas at 860 K the surface is found to be irregularly stepped (average separation 250 Å) [14]. Fe is deposited from a high purity wire by electron beam heating. Precise adjustment and continuous control of the flux are performed with an integrated flux monitor and a shutter. During growth the pressure does not exceed 1×10^{-10} mbar.

3. Computer simulation

In previous studies we have shown that angular distributions of fast ions which are grazingly scattered from surfaces can be adequately calculated by 3D binary collision computer simulations [14,21]. 25 keV He^+-ions with incidence angles Φ_{in} and Θ_{in} taken from experiment interact with a semi-infinite bcc Fe(1 0 0) target crystal. The trajectory of each ion is followed through a series of binary collisions with crystal atoms closest to the ion position. According to the experimental observable the fraction of ions scattered into a fixed small solid angle emulating the detector is evaluated.

In order to describe the real structure of the surface, we implement surface steps and thermal displacements of lattice atoms. Both have been found to affect angular distributions in characteristic ways. Inelastic processes leading to nuclear and electronic energy loss can be neglected. For details on the simulation program we refer to Ref. [14].

Growth is modeled by monatomic-height pseudomorphic islands (two-level model). This should be adequate for the initial stage of homoepitaxial growth on Fe(1 0 0) [15]. The distribution of island sizes and sizes of uncovered regions ("holes") is described either by a geometric distribution or a gamma distribution. The geometric distribution, which implies no interactions between steps (random distribution), is given by

$$P(n) = (1-\gamma)^{n-1}\gamma \quad (1)$$

with an average size $1/\gamma$ and n in units of the lattice constant [22]. Applying the theory of Markov chains, this is the obvious choice for our simulation method [13] and makes analytical solutions possible [23].

Typically the distribution of islands in growth processes is not random, because nucleation is less likely in the vicinity of existing islands [9]. A distribution which takes account of short-range interactions between steps and has a peak at some preferred size is the gamma distribution

$$P(n) = \frac{\alpha^M}{\Gamma(M)} e^{-\alpha n} n^{M-1} \quad (2)$$

with an average size M/α [24]. As M becomes large the gamma distribution approaches a normal distribution and in the extreme limit becomes a δ-function centered at M/α. Gamma distributions have been inferred from LEED for Ag/Si [4] and Fe/Au [2,3] with $M \approx 2$–3 being independent of coverage according to scale invariance. For homoepitaxy on Fe(1 0 0) the likelihood of a gamma distribution is deduced from an evaluation of STM-pictures [15] (Fig. 1) and its resemblance to simulation results [17].

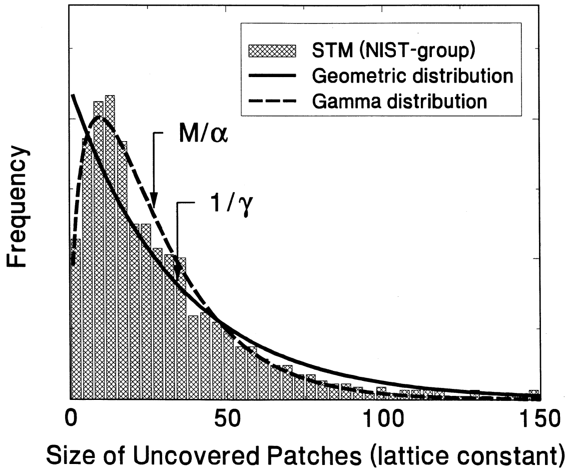

Fig. 1. Frequency distribution of sizes of uncovered patches ("holes") from an examination of an STM image (Fig. 1a in Ref. [15]) for 0.07 ML Fe grown on Fe(1 0 0) at 293 K. The lines are best fits for a geometric distribution ($\gamma = 0.029$) (solid line) and a gamma distribution ($M = 1.55$, $\alpha = 0.0575$) (dashed line). Roughly 1000 patches have been recorded for random lines of intersection around the [0 0 1] lattice direction.

4. Results

In Fig. 2 we compile 1D angular profiles of the specular beam recorded during growth of ≈ 1 ML Fe on Fe(1 0 0) at 440 K. The profiles change periodically when the surface cycles from flat to rough to flat [25]. Comparison of profiles for growth on a flat substrate surface (upper row) with profiles for a stepped substrate surface (lower row) [14] reveals that substrate steps and steps forming the boundary of islands affect the scattering process in different ways. A random sequence of up- and downward substrate steps results in a multilevel surface. In this case, angular profiles show a pronounced feature at small scattering angles caused by ions crossing (multiple) downward steps [14]. On the other hand, alternating up- and downward steps, as they appear for 2D growth, result in a symmetric broadening of the profiles. Thus, a mere inspection of the angular profile may serve as an indication whether a two-level growth model is appropriate or not.

In the simulations (Fig. 2, solid curves) we assume a geometric distribution of substrate steps, where up- and downward steps occur with equal probability. The average step separation is 4000 Å for the flat and 250 Å for the stepped substrate. Growth is modelled by a two-level geometric distribution with only one fit parameter, e.g. the average island separation $L = 1/\gamma$. The average island size then results from the coverage. All curves displayed in Fig. 2 are calculated with the same value $L = 90$ Å, i.e. the island density is constant. This well reproduces measured profiles in the aggregation regime. For larger coverages differences between experiment and simulation point to deviations from 2D growth due to nucleation on top of islands [10]. Consistent discrepancies in the high polar angle regime of the irregularly stepped substrate are attributed to scattering from defects, which are created during sputtering and do not disappear completely at annealing temperatures below 870 K [14].

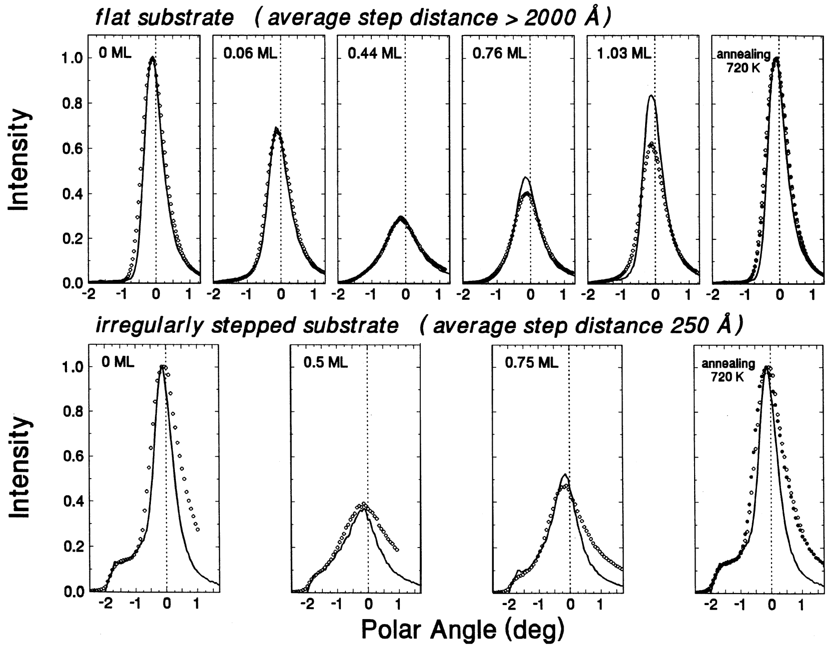

Fig. 2. Measured (circles) and simulated (curves) polar angular distributions for 25 keV He^+-ions scattered from Fe/Fe(1 0 0). The distributions are normalized to the maxima for the uncovered surface. Upper row: growth on a flat substrate surface (average separation of substrate steps >2000 Å); lower row: irregularly stepped surface (average separation 250 Å). The simulations were performed for a geometric distribution of island and hole sizes with a constant average island separation of 90 Å. The right-hand distributions (solid circles) were recorded after annealing the ≈ 1 ML Fe/Fe(1 0 0) surface at 720 K. Growth temperature: 440 K; deposition rate: 2.7×10^{-3} ML s^{-1} (upper row) and 4×10^{-3} ML s^{-1} (lower row).

The right-hand distributions in Fig. 2 (solid circles) are recorded after annealing the ≈ 1 ML films to 720 K. They are virtually indistinguishable from the pristine distributions for the uncovered surface (open circles). This shows that inter- and intralayer diffusion are sufficiently effective for a complete post-growth recovery of the film.

Fig. 3 shows the intensity in the maximum of the specular beam, recorded during growth at largely different temperatures and deposition rates. The lines represent fits to the measured oscillations for geometric (dotted lines) or gamma distributions (solid lines) of island separations. For an island density independent of coverage the number of fit parameters is reduced to one (α) also for the gamma distributions when M is set constant ($=3$), in accordance with Refs. [4,3]. Both distributions give fairly good fits. Deviations at small and large coverages are not surprising, since in these regimes island densities increase (decrease) due to nucleation (coalescence) of islands [10]. The low intensity observed for growth at low temperature (bottom curve) when approaching 1 ML indicates kinetic roughening, i.e. second layer growth sets in before the first layer is completed.

In the aggregation regime the island density is found to be roughly constant, just as observed by diffraction techniques [5,2,3,6]. Using gamma distributions and $L = 1/\sqrt{N}$ we infer for the data of Fig. 3 $N = 1.74 \times 10^{10}$, 9.47×10^{10}, and 2.37×10^{12} cm^{-2} from top to bottom. Geometric distributions yield larger values throughout $N = 2.12 \times 10^{10}$, 1.65×10^{11}, and 1.11×10^{13} cm^{-2}, respectively. Considering that a geometric and a gamma distribution with $M = 3$ should limit the range of realistic distributions, we conclude that the island density in the aggregation regime can be determined with good precision, unless N is very large, as for low temperatures and/or high deposition rates.

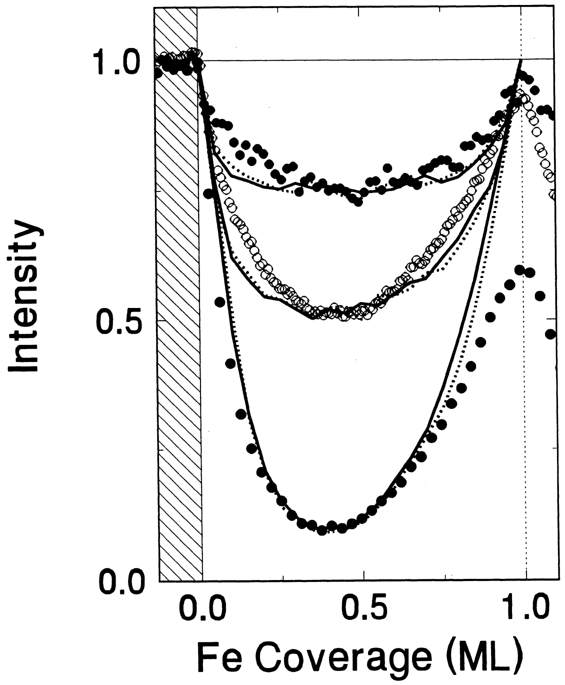

Fig. 3. Intensity of specularly reflected 25 keV He^+-ions (solid circles) recorded during homoepitaxial growth on Fe(1 0 0). The simulations are best fits for a geometric distribution of island and hole sizes (dotted curves) and a gamma distribution (solid curves). The average island separation is assumed to be independent of coverage (constant island density). Growth temperatures (from top to bottom): 590, 590, and 420 K; deposition rates: 9.0×10^{-3}, 5.75×10^{-2}, and 2.1×10^{-1} ML s^{-1}.

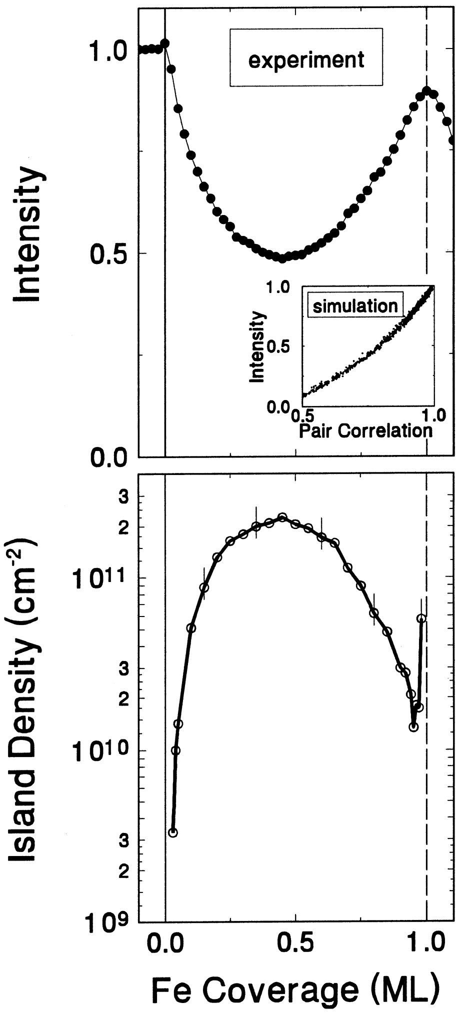

Fig. 4. Upper panel: intensity of specularly reflected 25 keV He^+-ions recorded during homoepitaxial growth on Fe(1 0 0) at 550 K and a deposition rate of 1.4×10^{-2} ML s^{-1}. Inset: calculated intensity of specularly reflected 25 keV He^+-ions versus pair correlation $C(10)$ for a geometric distribution of island and hole sizes and a growth temperature 550 K. Lower panel: island density vs. coverage as inferred from experiment and calculated calibration curve.

Without the constraint of a constant island density, one could estimate the coverage dependent island densities in Fig. 3 by piecewise fits. A less time consuming evaluation has been proposed in Ref. [13], where the specular-beam intensity has been found to be determined by the height correlation $C(n)$ between surface atoms separated by an effective ion-surface interaction length n. For geometric distributions the average island separation L can be calculated analytically from $C(n)$. An example is shown in Fig. 4. The evolution of the island density (bottom panel) resembles typical curves obtained from model calculations [10]. At low coverages the island density rapidly increases due to nucleation until it saturates leading to an extended aggregation regime, where the density is approximately constant. Finally, in the coalescence regime, the islands begin to join and percolate so that eventually nucleation and growth in the second layer sets in. The saturation island density $N = 2 \times 10^{11}$ cm^{-2} is in agreement with the saturation island density deduced from an STM study [15] for the same deposition rate and interpolation to the same growth temperature ($N = 2.6 \times 10^{11}$ cm^{-2}).

5. Summary

Grazing ion-surface scattering is an alternative to diffraction techniques to study epitaxial growth. It is a real-space technique applicable in situ and in real time even at high growth temperatures and deposition rates. Interpretation of measurements is straightforward by means of computer simulations emulating the ion trajectories within the framework of classical mechanics. Whereas basic information on the growth process is obtained by a mere inspection of intensity and angular profile of the specular beam, fits to experimental data yield morphological quantities like average island density and its dependence on coverage and growth parameters. Although the distribution of island size and separation is difficult of access, the predicted scale invariance [17] should allow one to deduce fundamental quantities like activation energies or critical island sizes by a systematic variation of growth temperature and deposition rate. Work on this subject is in progress.

Acknowledgements

The assistance of T. Igel and M. Ostwald in the experiments is gratefully acknowledged. This work was supported by the Deutsche Forschungsgemeinschaft (Sonderforschungsbereich 290).

References

[1] H.-J. Ernst, F. Fabre, J. Lapujoulade, Phys. Rev. B 46 (1992) 1929.
[2] Q. Jiang, A. Chan, G.-C. Wang, Phys. Rev. B 50 (1994) 11116.
[3] Q. Jiang, G.-C. Wang, Surf. Sci. 324 (1995) 357.
[4] J.-K. Zuo, J.F. Wendelken, Phys. Rev. Lett. 66 (1991) 2227.
[5] J.-K. Zuo, J.F. Wendelken, H. Dürr, C.-L. Liu, Phys. Rev. Lett. 72 (1994) 3064.
[6] H. Dürr, J.F. Wendelken, J.-K. Zuo, Surf. Sci. Lett. 328 (1995) L527.
[7] H.-J. Ernst, F. Fabre, R. Folkerts, J. Lapujoulade, J. Vac. Sci. Technol. A 12 (1993) 1809.
[8] W. Li, G. Vidali, O. Biham, Phys. Rev. B 48 (1993) 8336.
[9] J.A. Venables, G.D.T. Spiller, M. Hanbücken, Rep. Prog. Phys. 47 (1984) 399.
[10] J.G. Amar, F. Family, P.M. Lam, Phys. Rev. B 50 (1994) 8781.
[11] Y. Fujii, K. Narumi, K. Kimura, M. Mannami, T. Hashimoto, K. Ogawa, F. Ohtani, T. Yoshida, M. Asari, Appl. Phys. Lett. 63 (1993) 2070.
[12] T. Igel, R. Pfandzelter, H. Winter, Europhys. Lett. 35 (1996) 67.
[13] R. Pfandzelter, Surf. Sci. 421 (1999) 263.
[14] R. Pfandzelter, Phys. Rev. B 57 (1998) 15496.
[15] J.A. Stroscio, D.T. Pierce, R.A. Dragoset, Phys. Rev. Lett. 70 (1993) 3615.
[16] J.A. Stroscio, D.T. Pierce, Phys. Rev. B 49 (1994) 8522.
[17] J.G. Amar, F. Family, Phys. Rev. Lett. 74 (1995) 2066.
[18] J.G. Amar, F. Family, Phys. Rev. B 52 (1995) 13801.
[19] R. Pfandzelter, T. Igel, H. Winter, Surf. Sci. 375 (1997) 13.
[20] R. Pfandzelter, T. Igel, H. Winter, Surf. Sci. 389 (1997) 317.
[21] R. Pfandzelter, T. Hecht, H. Winter, Europhys. Lett. 44 (1998) 116.
[22] T.-M. Lu, M.G. Lagally, Surf. Sci. 120 (1982) 47.
[23] C.S. Lent, P.I. Cohen, Surf. Sci. 139 (1984) 121.
[24] P.R. Pukite, C.S. Lent, P.I. Cohen, Surf Sci. 161 (1985) 39.
[25] R. Pfandzelter, T. Igel, M. Ostwald, H. Winter, Appl. Surf. Sci. 142 (1999) 470.